Nanoscale

Accepted Manuscript

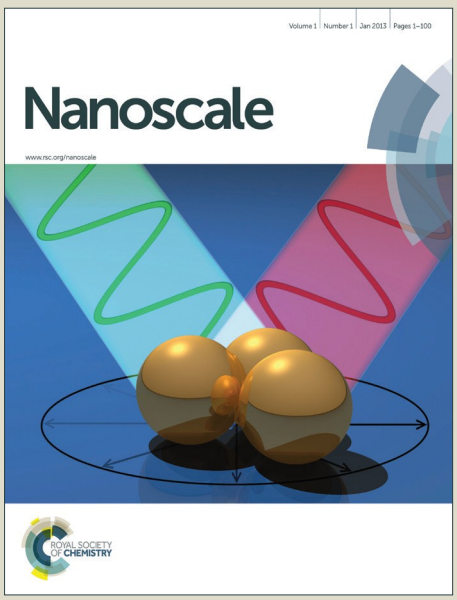

ROYAL SOCIETY OF CHEMISTRY

www.rsc.org/nanoscale

Cite this: DOI: 10.1039/c0xx00000x

www.rsc.org/xxxxxx

ARTICLE TYPE

Synthesis of nitrogen-doping carbon dots with different photoluminescent properties by controlling the surface states

Yun HuanYuan[a], Ze Xi Liu[b], Rong Sheng Li[b], Hong Yan Zou[b], Min Lin[b], Hui Liu,*[b] Cheng Zhi Huang*[ab]

Received (in XXX, XXX) XthXXXXXXXXX 20XX, Accepted Xth XXXXXXXXX 20XX

DOI: 10.1039/b000000x

Surface states of carbon dots (CDs) are critical to the photoemission properties of CDs. By carefully adjusting the reaction conditions in hydrothermal synthesis route, we have prepared a series of CDs with excitation-dependent emission (EDE) and excitation-independent emission (EIE) properties by controlling the content of nitrogen elements, proving that characteristic optical properties of CDs originate from their energy levels. It has been found that surface-passivation of the as-prepared CDs with nitrogen doping can improve the emission efficiency and be beneficial to EIE features due to the single electron transition resulting from the single functional groups. And the as-prepared CDs can specifically bind with Hg^{2+} with the emission quenched because of electrons transfer from the LUMO levels of CDs to Hg^{2+}.

Introduction

Carbon dots (CDs) have been attracting enormous attention due to their unique and novel properties. Because of their chemical stability, low photobleaching, less toxicity and biocompatibility[1-3], CDs have become new-generation photoluminescent (PL) nanomaterials with the excellent optical properties superior to conventionally used PL chromophores such as fluorescent organic small molecules (OSMs) and quantum dots (QDs)[4-6]. Until now, CDs have been demonstrated to be pretty good optical probes[1, 7, 8], and have been found wide applications in bioimaging[9-11], photocatalysis and energy conversion[12-14]. In order to prepare high quality of CDs with high emission ability and long-wavelength emission, efforts including laser ablation[15], electrochemical oxidation[12, 16], solid-phase method[17], microwave assisted methods and hydrothermal route[18-20] have been made so far. Reports on these issues are continuously increasing[21]. Thus understanding of the PL emission origins in CDs, controlling synthesis of various CDs with different optical properties, functionalizing the surface of CDs with various functional groups are still significant for further extending their applications.

Despite several PL emission mechanisms, such as CDs visible emission involvement of the size distribution[22] or surface states [23], radiation recombination of excitons and charge transfer[24], have been proposed, it is still hard to understand the emission origins because of lacking sufficient theoretical assumptions and experimental data on PL emission of CDs[22, 25]. One crucial issue is whether CDs can be controlled or chemically modified, like the succeeded modification and function of quantum dots, so as to tune their emissions and expand their applications[26]. Therefore, investigating CDs binding properties with either organic or inorganic ligands might be effective to explore the PL emission mechanisms of CDs and thus can further extend their applications[25].

As is known, CDs display with optical properties of either the excitation-dependent emission (EDE) or excitation-independent emission (EIE)[23]. It seems that most of CDs, particularly those prepared with natural raw materials such as orange, Bombyx mori silk, and eggs, have emissions in EDE features[9, 27, 28]. Comparatively, there are few reports about fluorescent CDs with the EIE features[29], and so their emission mechanism explorations are still seldom reported. All these facts inspired us to develop a rational strategy for controllable synthesis of CDs with EDE or EIE features and highly quantum yield in order to reveal the PL emission mechanisms of CDs.

In such case, we herein prepared a series of CDs with citric acid (CA), which acts as the carbon source, and guanidine hydrochloride, which acts as the N source, through a simple hydrothermal route. The guanidine hydrochloride used here in fact plays two roles, one acts as a N-doping precursor, and the other as a surface passivation agent[30]. It was found that the as-prepared CDs show emissions dependently or independently on the excitation wavelength (namely, from EDE to EIE features) with the increasing proportion of guanidine hydrochloride, and if the as-prepared CDs fully surface-passivized with adequate proportion of guanidine hydrochloride, the EIE features have high quantum yield up to 60.5%. In order to discern the PL mechanisms of CDs, we try to identify that the EIE mode and high QY of CDs could be governed by the surface states of CDs. Further identifying is that the unpaired electrons of the amine functional groups in CDs can contribute to the electron donation of the CDs and improve the emission properties, because it is more likely to transit from the ground state to the lowest excited singlet state of the electrons [4, 25, 31].

In order to investigate the surface states of the as-prepared CDs, binding investigations between the CDs with a variety of metals ions were made , because CDs synthesized with different

carbon sources materials have different binding ability with metal ions such as iron (III) ions, copper (II) ions, and mercury (II) ions[2, 32, 33], wherein PL quenching is generally occurred. The highly specific binding ability of the as-prepared CDs with mercury (II) ions was identified to be dependent on surface states, which could be attributed to different HOMO/LUMO energy levels of CDs. Furthermore, the specific binding of CDs to mercury (II) ion shows that the CDs can serve as an effective fluorescent probe for specifically visual monitoring of intracellular mercury (II) ions.

Experimental

Apparatus

UV-vis absorption and PL emission features of CDs were characterized by a Hitachi UV-3600 spectrophotometer (Tokyo, Japan) and a Hitachi F-2500 fluorescence spectrophotometer (Tokyo, Japan), respectively. The Raman spectrum was measured with LabRAM HR800 Laser confocal Raman spectrometer (Horiba JobinYvon Inc., France) at ambient temperature (about 25 ^{o}C) on an Ag substrate. The fluorescence life time was obtained with FL-TCSPC fluorescence spectrophotometer (Horiba JobinYvon Inc., France). High-resolution TEM (HRTEM) images and fast Fourier transform (FFT) spot diagrams of the CDs were recorded with a high resolution transmission electron microscope (Tecnai G2 F20 S-TWIN, FEI Company, USA) operating at 200 kV. X-ray diffraction (XRD) pattern was recorded with a Rigaku Ultima IV instrument (Tokyo, Japan). Elemental and functional groups analysis was performed on a Thermo escalab 250Xi X-ray photoelectron spectrometer (USA) and a Shimadzu FTIR-8400S Fourier transform infrared spectrometer (Kyoto, Japan), respectively. Fluorescence imaging was operated on an Olympus DSU live-cell confocal microscope (Tokyo, Japan) system with laser excitations of DAPI.

Synthesis of photoluminescent carbon dots

Typically, the CDs were prepared by uniformly mixing 0.0875 g citric acid (CA) and 0.48 g guanidine hydrochloride at first and then the mixture was dissolved into 10.0 mL NaOH (1 g/100 mL). The mixture then incubated at 180 ^{o}C for 2 h in a 25 mL Teflon-lined stainless steel autoclave. With the reaction completion, the autoclave was naturally cooled to room temperature, and the aqueous solution was then centrifuged at 12000 rpm for 15 min to discard the non-fluorescent deposit. The upper CDs aqueous solution was collected and dialyzed through a membrane (1000 MWCO) over 24 h to remove the residual citric acid and guanidine hydrochloride. The obtained CDs were finally concentrated at −80^{o}C and dried under vacuum.

Cytotoxicity investigations

In order to extend the bioapplications of the as-prepared CDs, a serial of biosafety tests should be made. Human epidermoid cancer cells (Hep-2) were used to evaluate the cytotoxicity of the as-prepared CDs through through Cell Counting Kit-8(CCK-8) method[3]. Briefly, 100 μL of 1.0×10^{5} cells / mL human epidermoid cancer cells (Hep-2) in Roswell Park Memorial Institute 1640 medium (RPMI 1640) supplemented with 2% fetal bovine serum were added to each well of a 96-well plate. The cells were cultured first for 24 h in an incubator (37 ^{o}C, 5% CO_2), and for another 24 h of being cultured with the 90 μL of Roswell Park Memorial Institute 1640 medium (RPMI 1640) containing 10 μL of the CDs with different concentrations (0, 0.2, 0.4, 0.6, 0.8, 1 mg mL^{-1}). After removing the culture medium, the cells washed with PBS buffer twice, and then 10 μL of Cell Counting Kit-8 (CCK-8) solution was added to every cell well, in which 90 μL RPMI 1640 contained. The cells were further incubated for 0.5 h. The optical density (OD) of the mixture was recorded with a Microplate Reader Model at 450 nm. The cell viability values were determined (at least three times) based on the following equation:

$$C_{\mathrm{v}} = \frac{OD_{\mathrm{treated}}}{OD_{\mathrm{control}}}$$

Wherein C_{v} is the cell viability (%), OD_{control} is the optical density and could be obtained in the absence of CDs, while OD_{treated} obtained in the presence of CDs.

Binding features of CDs with metal ions

The binding features of CDs with metal ions were performed in Tris-HCl (pH 7.0) buffer solution at room temperature. In a typical run, 0.10 mL Tris-HCl buffer (pH 7.0) and 0.10 mL CDs were added into a 2.0 ml EP tube at first. After the addition of metal ions, the mixture was mixed fully, and then diluted to 1.0 ml with doubly distilled water with blending thoroughly. 10 min later, the mixture was then transferred to measure PL emission features at room temperature.

Intracellular uptake experiments of Hg^{2+}

In order to observe the intracellular uptake of Hg^{2+} through its specific binding with CDs, the Hep-2 cells in RPMI 1640 supplemented with 10% fetal bovine serum employed, which were added to each well of a 24-well plate (300 μL per well) at first. The cells were cultured then for 24 h in an incubator (37 ^{o}C, 5% CO_2), and for another 12 h after the culture medium was replaced with 270 μL of RPMI 1640 containing 30 μL CDs (at the concentration of 1 mg mL^{-1}). Following the removal of the culture medium, each well was washed with PBS buffer for three times, and then mounted with glycerol on microscope slides for imaging.

Results and discussion

Preparation and characterizations of N-CDs

The preparation of CDs was conducted by directly condensing the citric acid and guanidine hydrochloride in the medium of NaOH solution, during which polymer-like CDs were formed at first, and then carbonized to high content nitrogen CDs[29]. As Fig.1 shows, the as-prepared CDs are well-dispersed and have a uniform size distribution between 3 and 6 nm with an average

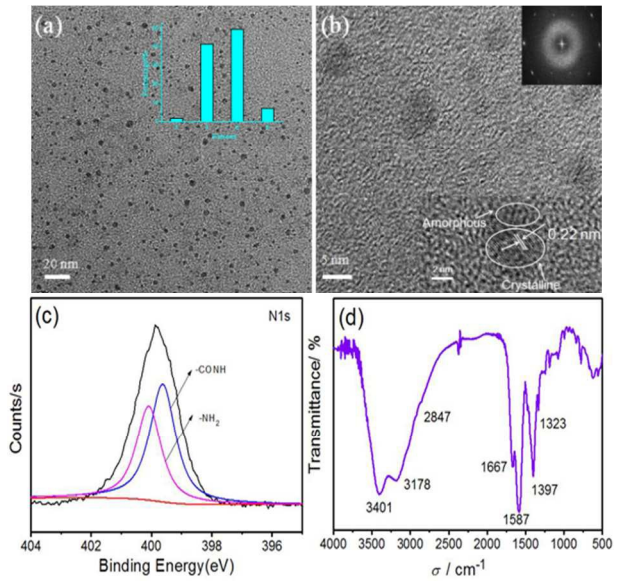

Fig.1 The morphology and compositions of the CDs (a) TEM image of CDs and (b) HRTEM images of the CDs. Inset: size distribution (the size distribution histogram was obtained by statistical analysis of more than 100 particles) and FFT image of the CDs. (c) High-resolution N 1s spectra and (d) FTIR spectrum of the products.

diameter of about 4.61 nm (Fig.1a). High resolution TEM (HRTEM) image (Inset of Fig. 1b) clearly reveals the presence of both crystalline graphite and amorphous phases, and the lattice spacing of 0.22 nm are well consistent with the (100) facet of graphitic carbon[22]. XRD pattern displays highly disordered amorphous carbon of CDs (Fig. S1, ESI†), and the Raman spectrum suggests the existence of defects in the CDs (Fig. S2, ESI†). All results imply that the as-prepared CDs are composed of nanocrystalline cores of graphitic sp^2 carbon atoms and sp^3 carbons defects in the cores or on the surfaces.

High-resolution N 1s spectra reveal that N exists in the forms of aromatic N (399.6 eV) and surface H_2N- groups (400.1 eV) in the CDs[34] (Fig.1c). The FTIR spectrum displays several absorption peaks related to the surface functional groups of the CDs. The absorption peaks at 3401 cm^{-1} and 1587cm^{-1} can be assigned to the -NH groups, while the absorption peaks at 1667 cm^{-1} and 1323 cm^{-1} are attributed to C=O stretching vibrations and O–H bending vibration, respectively[35] (Fig.1d). The aromatic N and C=O bonds observed by XPS and FTIR indicate that the amide bonds have formed, which might be ascribed to the dehydration and condensation reactions between carboxyl and amino-groups[29], indicating that guanidine hydrochloride acts as N-dopant and surface passivation agent, and thus greatly contributing to the formation of CDs with high PL emission efficiency.

The remarkable optical properties of the as-prepared CDs have two typical absorption bands characterized at 234 nm and 332 nm, respectively (Fig. 2a). The 234 nm band is consistent with the $\pi \rightarrow \pi^*$ transition of C=C, while the strong absorption band at 332 nm could be attributed to $n \rightarrow \pi^*$ transition of surface groups[36]. The maximum excitation wavelength is located at 363 nm, which is consistent with the UV–vis absorption spectrum characterized at 332 nm, giving an emission band characterized at 460 nm. That is to say, the wavelength of the absorption peak of CDs is almost

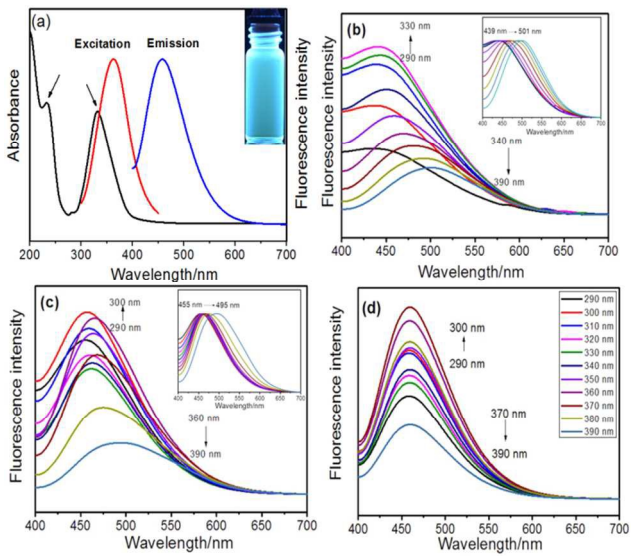

Fig.2 UV–vis absorption and PL spectra of the CDs. (a) The emission spectrum was obtained under maximum excitation at 363 nm, and the excitation spectrum was obtained at the maximum emission wavelength of 460 nm. Inset: photograph taken under 365nm UV light (CDs-6) (b) CDs-1 and (c) CDs-3 at different excitation wavelengths. Inset: the normalized PL emission spectra. (d) Emission spectra of CDs-6 under different excitation wavelengths.

the same as that of the excitation peak of CDs, implying that nonradiative transition has scarcely occurred in the CDs [30].

Recent investigations have made the excitation wavelength-dependent emission (EDE) well established[2, 37], and it seems that surface modification or surface passivation can prompt the excitation-independent emission (EIE) features[37]. To further identify the surface passivation mechanism, we investigated the role of amine groups in which the nitrogen atom has been generally employed to passivate the functional groups on the surface of CDs in the hydrothermal route[31]. By preparing a serials of CDs with different molar ratios of citric acid and guanidine hydrochloride (Table 1 and ESI†), named as CDs-1, CDs-2, CDs-3, CDs-4, CDs-5 and CDs-6, respectively, which the nitrogen content changes from 5.5% to 19.9%, we then measured their PL features including the emission wavelength and emission lifetime, and found that the emission wavelengths of CDs-1, CDs-2 and CDs-3 (Fig.2b, Fig.S4 and Fig.2c) depend on the excitation wavelengths, and then gradually shift to long wavelength with increasing excitation wavelength. In contrast, CDs-4, CDs-5 and CDs-6 show excitation-independent emission (EIE) (Fig.2d, Fig.S5 and Fig. S6).

This nitrogen content-dependent emission features can be explained by surface energy levels of CDs[23]. For the EDE CDs including CDs-1, CDs-2 and CDs-3, there are diverse surface groups, such as C=C–C=O and C=O (Fig. S8, ESI†), which can introduce trapping states with a series of energy levels, making CDs emit photons that vary with excitation energy[15]. It has demonstrated that the surface state of CDs is analogous to a molecular state[29], wherein various surface states correspond to a relatively wide distribution of different energy levels, enlarging the excitation wavelength range and causing the EDE[2]. In contrast, there are only single energy levels if surface states are completely passivated with amino-groups[29], resulting in EIE features. The EIE features of CDs-4, CDs-5 and CDs-6 show that

Table 1 | Fluorescence lifetime and quantum yield (QY) of CDs with different content of nitrogen

No	CDs-1	CDs-2	CDs-3	CDs-4	CDs-5	CDs-6
N%	5.5	12.0	12.3	16.0	19.0	19.8
λem(nm)	442	458	458	443	458	460
τ_1 (ns)	2.5 (24.2 %)	3.8 (37.9 %)	5.8 (60.3 %)	6.6 (100.0 %)	7.9 (100.0 %)	7.5 (100.0 %)
τ_2(ns)	6.6 (32.1 %)	13.5 (32.07 %)	11.6 (23.3 %)			
τ_3(ns)	16.5 (19.1 %)	0.63 (30.03 %)	0.8 (16.4 %)			
τ_4(ns)	0.8 (24.6 %)					
τ_{ave}(ns)	6.0	6.0	6.3	6.6	7.9	7.5
QY%	3.4	6.3	11.7	13.6	53.7	60.5

Excitation, 370 nm excitation.

single energy levels on their surface because of the passivation by amino-groups, making the single electron transition of energy levels.

Further measurements of fluorescence lifetime can also illustrate that the content of nitrogen is critical to the emissions of EIE or EDE features. The decay curves of the CDs-1, CDs-2 and CDs-3 could be best fitted with a three-exponential decay or a four-exponential decay, while CDs-4, CDs-5, and CDs-6 only exhibit a single-exponential function (Table 1), giving significant evidence that the fluorescence lifetime is dependent on the content of nitrogen. As Table 1 shows, multiple lifetimes are involved for those of CDs with low content of nitrogen, while single lifetimes involved for those of CDs with high content of nitrogen, indicating that diverse fluorophores or various energy levels lead the formation of a variety of radiative transitions[23]. So, it is obviously that electron-donating amino-group, which can enhance the passivation degree of traps on CDs[29], leads to a single energy level and excitation-independent behavior. In such case, we can control the surface states by changing the density of amino-groups on the surface of CDs, making the CDs emissive either with excitation dependence or independence.

Table 1 further shows that CDs-6, which contains 19.8% of nitrogen, has a fluorescence lifetime of 7.5 ns (Table 1 and Fig.S7, ESI†), exhibiting excellent PL behavior with a highly relative quantum yield (QY) of 60.5 %, which is higher than other materials, thus CDs-6 own highest photoluminescence efficiency among the CDs. Such short lifetime and high photoluminescence efficiency indicate that radiative recombination of the surface-trapped electrons and holes in CDs-6 are responsible for the fluorescence emissions[37]. In order to well understand the high emissive features of CDs-6, we turn back to further investigating the FTIR features of the functional groups on the surfaces of these CDs. It was shown (Fig. S8, ESI†) that CDs-6 has pretty strong absorption band of –NH at 1587cm^{-1}, as accompanied to the weak absorption band of –NH of other CDs. Owing to the

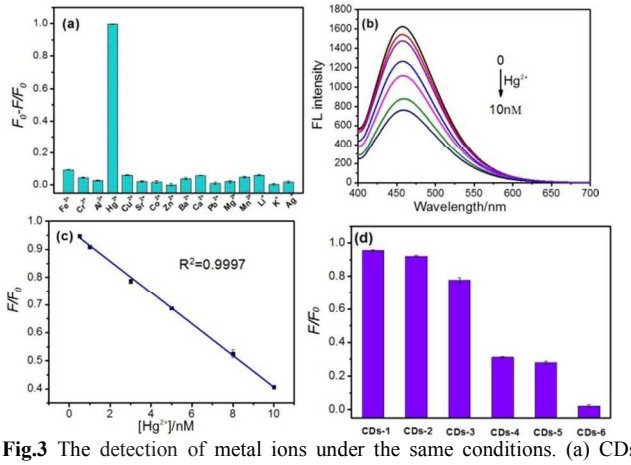

Fig.3 The detection of metal ions under the same conditions. (a) CDs selective bind with different ions. (b) Emission spectra of CDs in the presence of different concentrations of Hg^{2+} and (c) the linear relationship between the PL intensity and Hg^{2+} concentration in the range of 0.5nM and 10nM, and there was a great linear calibration plot expressed as $(F_0\text{-}F)/F_0$=-0.056c+0.97with a correlation coefficient of 0.9997. (d) The changes of FL intensity for different CDs binding with 100 nM Hg^{2+}.

passivation of these CDs by –NH group, the absorption of C=O at 1667 cm^{-1} got weaker and weaker (CDs-3, CD-4, CD-5 and CD-6) with the increase of–NH group and so it is hardly observed the absorption of C=O at 1667 cm^{-1} of CD-6. Meanwhile, CDs-1 and CDs-2 display extremely weak absorption band of amide bond, corresponding to their low emission efficacy, and thus implying the abundant amino-groups may contribute to the highly quantum yield. That is to say, the high PL emission comes from the amino groups on the CDs surface, resembling the PL mechanism of organic dye. In other words, the amino-groups can enhance the conjugation degree of conjugated systems, which then increase the electron transition probability from the ground state to the lowest excited singlet state, and thus contribute to higher QY indirectly of the CDs. Moreover, it is reasonable to believe that the doping of nitrogen can make the CDs be a new kind of state, making the electrons trapped by the new formed surface states, which facilitate a high yield of radiative recombination. So, nitrogen-doped surface states facilitate a high yield of radiative recombination and depress non-radiativere combination[25].

Highly specific interaction between CDs and Hg^{2+}ions

In order to understand the PL emission features, we further investigated the binding features of CDs with metals ions because there are a lot of the functional groups of carboxyl and amino-groups on the surface of CDs, which are easily bound with metal ions.

Fig. 3a shows that the PL emissions of CDs-6 could be specifically quenched by Hg^{2+}, and other metal ions including Fe^{3+}, Cr^{3+}, Al^{3+}, Cu^{2+}, Cd^{2+}, Co^{2+}, Zn^{2+}, Ba^{2+}, Ca^{2+}, Pb^{2+}, Mg^{2+}, Ni^{2+}, Li^{+}, Na^{+} and Ag^{+} can scarcely quench the PL emissions of CDs-6. The excellent specificity of CDs-6 binding with Hg^{2+} even if the concentration lower than 0.12 nM, which could be probably attributed to the binding between Hg^{2+} and carboxyl or hydroxyl groups, making the electrons transfer occurs from the CDs to Hg^{2+}. Measurement of the UV–vis absorption spectrum showed that a blue shift of the characteristic absorption of CDs-6 at 332

nm to 326 nm occurred after interacting with Hg^{2+}, indicating that Hg^{2+} could make the electronic structure of CDs changed (Fig. S13, ESI†). Since Hg^{2+} ions have the highest binding constant (K_f) with carboxyl of all these tested metal ions (Cu^{2+}, Cd^{2+}, Co^{2+}, Pb^{2+}, Ni^{2+}, and Ag^{+}), so we suppose that the specific quenching of CDs by Hg^{2+} ions might be ascribed to the binding of Hg^{2+} ions with the carboxyl on the surface of CDs, identical to the finding of refs[31].

As shown in Fig. 3b, the FL intensity of CDs-6 at 460 nm decreased gradually with increasing the concentration of Hg^{2+} from 0.5 nM to 10 nM. And there was a good linear calibration plot over the concentration range of 0.5–10 nM with a correlation coefficient of 0.9997 (Fig. 3c), with a limit of detection as low as 0.12 nM (3σ), which is much lower than other previously reported values[38]. These results indicate that the as-prepared CDs-6 could be employed as a much more sensitive optical probe than previously reported optical ones. It is noticeable that hydrothermal synthesis route does not need expensive reagents, not need complex operations procedures and further surface modification. In other word, the prepared CDs-6 is very suitable to be applied for monitoring and detection of Hg^{2+}.

The sensitive binding feature between CDs-6 with Hg^{2+} excited our curiosity to further investigate their binding mechanism. TEM images of the as-prepared CDs show that average size of the CDs get enlarged from 4.61 nm to 16.2 nm after interacting with Hg^{2+}, indicating that some degree of aggregations has occurred (Fig.1a and Fig. S14, ESI†). Then, the highest occupied molecular orbital (HOMO) and lowest unoccupied molecular orbital (LUMO) energy levels of CDs could be estimated by the empirical formula,[29, 39]

$$E_{HOMO} = -e\,(E_{ox} + 4.4) \quad (1)$$

$$E_{LUMO} = -e\,(E_{red} + 4.4) \quad (2)$$

wherein E_{ox} and E_{red} are the onset of oxidation and reduction potential for CDs-6, respectively. The E_{red} was measured as −0.36 eV, as showed by cyclic voltammograms in solution (Fig. S16, ESI†), then the corresponding ELUMO was calculated to be −4.04 eV. By combing the E_{red} with the optical energy band gap (Eg), HOMO levels can be calculated,

$$E_{HOMO} = E_{LUMO} - E_g \quad (3)$$

wherein the E_g results from the absorption edge in the absorption spectrum, and was estimated to be 2.91 eV. Thus, the E_{HOMO} was calculated to be −6.95 eV.

In the same way, we can measure and calculate the E_{HOMO} and E_{LUMO} data of other CDs (Scheme 1). It could be seen that the HOMO/LUMO band gap of the CDs prepared by this hydrothermal synthesis route (including CDs-2, CDs-3, CDs-4, CDs-5, and CDs-6) overlaps with the mercury (II) ion redox potential. If Hg^{2+} was present, the electrons transfer occurs from the LUMO levels of CDs to Hg^{2+}, instead of transferring to HOMO levels[40], leading to CDs fluorescence quenching. The HOMO/LUMO band gap of the C-Dots-based materials overlaps with the mercury (II) ion redox potential, so the electrons transfer from CDs to mercury (II) ion[40]. Therefore, we suppose that the Hg^{2+}-mediated FL quenching of N-doped C-Dots exist in the electron transfer overlapping (Scheme 1). That is to say, the fluorescence quenching of CDs by Hg^{2+} is contribute to the electrons transfer from the LUMO levels of CDs to Hg^{2+}, and the N-doped modulates the chemical and electronic characteristics of the CDs, making the electrons transfer from CDs to Hg^{2+} effectively. Because amino-groups affect the chemical and electronic structure of carbon, thus LUMO of CDs-6 is much closer to the redox potential of mercury (II) ion than other CDs, so the electrons of CDs transfer to Hg^{2+} more easily.

Intracellular Imaging of Hg^{2+}

As shown in Figure 4, the cells show strong bright blue-green fluorescence after incubated with CDs for 12 h, suggesting that CDs successfully and efficiently got into cells via endocytosis[41]. Further experiments were performed by treating Hep-2 cells with different concentrations of Hg^{2+} to semiquantitative visualization and monitoring the intracellular Hg^{2+} level (the cells treated with PBS and 0 nM, 1 nM, 5 nM and 10 nM Hg^{2+} for one decreased with the increase of Hg^{2+} concentration, and the laser confocal microscopic images are consistent with quantitative analysis of fluorescence intensity (Fig.S17, ESI†), indicating that our probe could be applied for trace monitoring the intracellular Hg^{2+}.

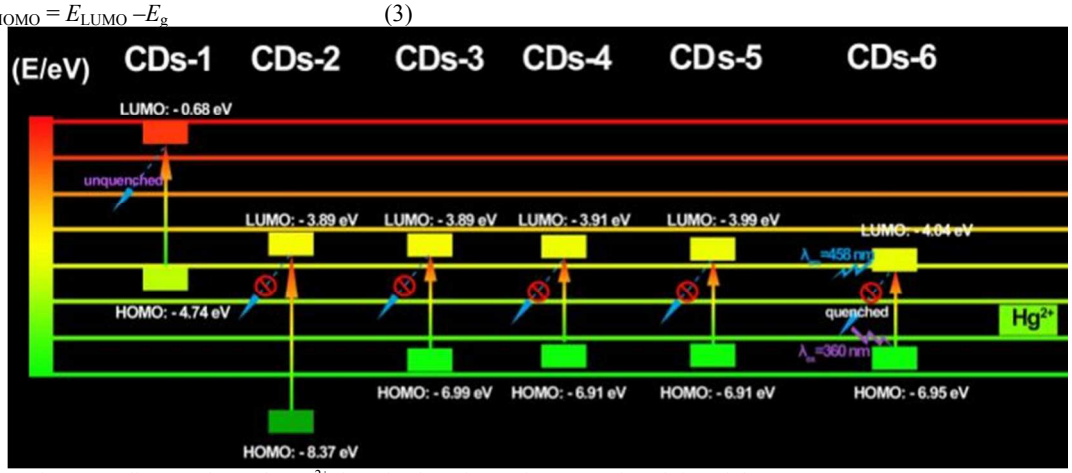

Scheme 1 Schematic energy diagram shows the Hg^{2+} detection by using various CDs (from left to right: CDs-1, CDs-2, CDs-3, CDs-4, CDs-5 and CDs-6), explaining by the probability of the e^- transfer mechanism.

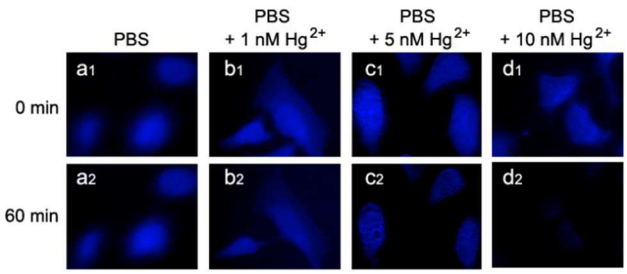

Fig.4 Laser confocal microscopic images of Hep-2 cells in each group of cell.Hep-2 cells incubated with CDs for 12 h, then treated with PBS for 0 and 60 min (a_1 and a_2), PBS and 1 nM Hg^{2+} for 0 and 60 min (b_1 and b_2), PBS and 5 nM Hg^{2+} for 0 and 60 min (c_1 and c_2) and PBS with 10 nM Hg^{2+} for 0 and 60 min (d_1 and d_2).

Conclusions

Consequently, different types C-Dots-based materials excitation-independent and excitation-dependent fluorescent materials have been prepared by an easy bottom–up route. By controlling the molar ratios of CA and guanidine hydrochloride, different surface density of amino-groups of the materials were obtained. By detailed work, it is found that the surface states could be completely passivated by amino-groups, leading to single energy level and exhibiting highly luminescence. In addition, the materials can be used to detect mercury ions with good selectivity and sensitivity, and have been applied to semiquantitative monitoring of the intracellular Hg^{2+} level, demonstrating the CDs have potential value for biological and biomedical research. We deeply believe that such adjustable fluorescent materials could be potentially unitized for optical devices, bioimaging, and energy conversion.

This work was financially supported by the National Natural Science Foundation of China (No. 21535006) and the Ministry of Science and Technology of the People's Republic of China (2011CB933600).

Notes and references

[a] *Key Laboratory on Luminescence and Real-Time Analytical Chemistry, Ministry of Education, College of Chemistry and Chemical Engineering, Southwest University, Chongqing 400715, China. E-mail: chengzhi@swu.edu.cn; Fax: +86 23 68367257; Tel: +86 23 68254659*

[b] *College of Pharmaceutical Science, Southwest University, Chongqing 400716, China. E-mail: liuhui78@swu.edu.cn; Fax: +86 23 68367257; Tel: +86 23 68254659*

† Electronic Supplementary Information (ESI) available: [details of any supplementary information available should be included here]. See DOI: 10.1039/b000000x/

1. J. Ju and W. Chen, *Anal. Chem.*, 2015, **87**, 1903-1910.
2. K. Hola, Y. Zhang, Y. Wang, E. P. Giannelis, R. Zboril and A. L. Rogach, *Nano Today*, 2014, **9**, 590-603.
3. Y. H. Yuan, R. S. Li, Q. Wang, Z. L. Wu, J. Wang, H. Liu and C. Z. Huang, *Nanoscale*, 2015, **7**, 16841-16847.
4. M. X. Gao, C. F. Liu, Z. L. Wu, Q. L. Zeng, X. X. Yang, W. B. Wu, Y. F. Li and C. Z. Huang, *Chem. Commun.*, 2013, **49**, 8015-8017.
5. Z. L. Wu, M. X. Gao, T. T. Wang, X. Y. Wan, L. L. Zheng and C. Z. Huang, *Nanoscale*, 2014.
6. S. Chen, J.-W. Liu, M.-L. Chen, X.-W. Chen and J.-H. Wang, *Chem. Commun.*, 2012, **48**, 7637-7639.
7. H. X. Zhao, L. Q. Liu, Z. D. Liu, Y. Wang, X. J. Zhao and C. Z. Huang, *Chem. Commun.*, 2011, **47**, 2604–2606.
8. X. Gao, Y. Lu, R. Zhang, S. He, J. Ju, M. Liu, L. Li and W. Chen, *J. Mater. Chem. C*, 2015, **3**, 2302-2309.
9. Z. L. Wu, P. Zhang, M. X. Gao, C. F. Liu, W. Wang, F. Leng and C. Z. Huang, *J. Mater. Chem.B*, 2013, **1**, 2868-2873.
10. M. Nurunnabi, Z. Khatun, K. M. Huh, S. Y. Park, D. Y. Lee, K. J. Cho and Y.-k. Lee, *ACS Nano*, 2013.
11. Y. Liu, Y. Xu, Y. Tian, C. Chen, C. Wang and X. Jiang, *Small*, 2014, **10**, 4505-4520.
12. H. Li, X. He, Z. Kang, H. Huang, Y. Liu, J. Liu, S. Lian, C. H. A. Tsang, X. Yang and S.-T. Lee, *Angew. Chem. Int. Ed.*, 2010, **49**, 4430-4434.
13. S. Chandra, P. Patra, S. H. Pathan, S. Roy, S. Mitra, A. Layek, R. Bhar, P. Pramanik and A. Goswami, *J. Mater. Chem. B*, 2013, **1**, 2375-2382.
14. D. Qu, M. Zheng, P. Du, Y. Zhou, L. Zhang, D. Li, H. Tan, Z. Zhao, Z. Xie and Z. Sun, *Nanoscale*, 2013, **5**, 12272-12277.
15. J. Shang, L. Ma, J. Li, W. Ai, T. Yu and G. G. Gurzadyan, *Sci. Rep.*, 2012, **2**, 792.
16. J. Zhou, C. Booker, R. Li, X. Zhou, T.-K. Sham, X. Sun and Z. Ding, *J. Am. Chem. Soc.*, 2007, **129**, 744-745.
17. J. Zhou, Y. Yang and C.-y. Zhang, *Chem. Commun.*, 2013, **49**, 8605-8607.
18. W. Shi, X. Li and H. Ma, *Angew. Chem. Int. Ed.*, 2012, **124**, 6438-6541.
19. X. Jia, J. Li and E. Wang, *Nanoscale*, 2012, **4**, 5572-5575.
20. L. Song, J. Shi, J. Lu and C. Lu, *Chem. Sci.*, 2015, **6**, 4846-4850.
21. J. Kim and J. S. Suh, *ACS Nano*, 2014, **8**, 4190-4196.
22. S. N. Baker and G. A. Baker, *Angew. Chem. Int. Ed.*, 2010, **49**, 6726-6744.
23. H. Nie, M. Li, Q. Li, S. Liang, Y. Tan, L. Sheng, W. Shi and S. X.-A. Zhang, *Chem. Mater.*, 2014, **26**, 3104-3112.
24. S. H. Jin, D. H. Kim, G. H. Jun, S. H. Hong and S. Jeon, *ACS Nano*, 2012, **7**, 1239-1245.
25. Y. Dong, H. Pang, H. B. Yang, C. Guo, J. Shao, Y. Chi, C. M. Li and T. Yu, *Angew. Chem. Int. Ed.*, 2013, **52**, 7800-7804.
26. F. M. Winnik and D. Maysinger, *Acc. Chem. Res.*, 2013, **46**, 672-680.
27. J. Wang, C.-F. Wang and S. Chen, *Angew. Chem. Int. Ed.*, 2012, **124**, 9431 –9435.
28. S. Sahu, B. Behera, T. K. Maiti and S. Mohapatra, *Chem. Commun.*, 2012, **48**, 8835-8837.
29. S. Zhu, Q. Meng, L. Wang, J. Zhang, Y. Song, H. Jin, K. Zhang, H. Sun, H. Wang and B. Yang, *Angew. Chem. Int. Ed.*, 2013, **125**, 4045-4049.
30. L. Shen, L. Zhang, M. Chen, X. Chen and J. Wang, *Carbon*, 2013, **55**, 343-349.
31. Y. Guo, Z. Wang, H. Shao and X. Jiang, *Carbon*, 2013, **52**, 583-589.
32. L. Zhou, Y. Lin, Z. Huang, J. Ren and X. Qu, *Chem. Commun.*, 2012, **48**, 1147-1149.
33. W. Lu, X. Qin, S. Liu, G. Chang, Y. Zhang, Y. Luo, A. M. Asiri, A. O. Al-Youbi and X. Sun, *Anal. Chem.*, 2012.
34. Y. Yang, J. Cui, M. Zheng, C. Hu, S. Tan, Y. Xiao, Q. Yang and Y. Liu, *Chem. Commun.*, 2012, **48**, 380-382.
35. X. Zhai, P. Zhang, C. Liu, T. Bai, W. Li, L. Dai and W. Liu, *Chem. Commun.*, 2012, **48**, 7955-7957.
36. M. Liu and W. Chen, *Nanoscale*, 2013, **5**, 12558-12564.
37. S. Y. Lim, W. Shen and Z. Gao, *Chem. Soc. Rev.*, 2015, **44**, 362-381.
38. R. Zhang and W. Chen, *Biosens. Bioelectron.* , 2014, **55**, 83-90.
39. H. Zhang, Y. Chen, M. Liang, L. Xu, S. Qi, H. Chen and X. Chen, *Anal. Chem.*, 2014, **86**, 9846-9852.
40. N. Vilar-Vidal, J. Rivas and M. A. Lopez-Quintela, *Phys. Chem. Chem. Phys.*, 2014, **16**, 26427-26430.
41. P. Rivera_Gil, M. Nazarenus, S. Ashraf and W. J. Parak, *Small*, 2012, **8**, 943-948.